Heterogeneous Environment of the S−H Group of Cys966 near the Flavin Chromophore in the LOV2 Domain of *Adiantum* Neochrome1

Yoshiaki Sato,[‡] Mika Nabeno,[§] Tatsuya Iwata,[‡] Satoru Tokutomi,[||] Minoru Sakurai,[§] and Hideki Kandori*,[‡]

Department of Materials Science and Engineering, Nagoya Institute of Technology, Showa-ku, Nagoya 466-8555, Japan, Center for Biological Resources and Informatics, Tokyo Institute of Technology, Midori-ku, Yokohama 226-8501, Japan, and Department of Biological Science, Graduate School of Science, Osaka Prefecture University, Sakai, Osaka 599-8531, Japan

Received May 25, 2007; Revised Manuscript Received July 14, 2007

ABSTRACT: The primary photochemistry of the blue-light sensor protein, phototropin, is adduct formation between the C4a atom of the flavin mononucleotide (FMN) chromophore and a nearby, reactive cysteine (Cys966), following decay of the triplet excited state of FMN. The distance between the C4a position of FMN and the sulfur atom of Cys966 is 4.2 Å in the LOV2 domain of *Adiantum* neochrome 1 (neo1-LOV2), a fusion protein of phototropin containing the phytochrome chromophoric domain. We previously reported the presence of an unreactive fraction in neo1-LOV2 at low temperatures, which presumably originated from the heterogeneous environment of Cys966 [Iwata, T., Nozaki, D., Tokutomi, S., Kagawa, T., Wada, M., and Kandori, H. (2003) *Biochemistry 42*, 8183−8191]. The present study showed that (i) 28% forms an adduct at 77 K (state I), (ii) 50% forms an adduct at 150 K but not at 77 K (state II), and (iii) 22% does not form an adduct at 150 K (state III). By Fourier transform infrared (FTIR) spectroscopy, we observed the S−H stretching frequencies at 2570 and 2562 cm^{-1} for state I and at 2563 cm^{-1} for state II, suggesting that the microenvironment of the S−H group of Cys966 determines the reactivity at low temperatures. Adduct formation is more efficient for state I than for states II and III. Molecular dynamics simulation strongly suggests that the observed multiple structures originate from the isomeric forms of Cys966. We thus concluded that there are multiple local structures of FMN and cysteine in neo1-LOV2, each of which is thermally converted by protein fluctuation at physiological temperatures.

It has been known for a long time that biological light-signal transduction can be initiated by cis−trans photoisomerization of a chromophore. In fact, photoisomerization of retinal, phytochromobilin, and *p*-coumaric acid takes place in rhodopsins (*1*), phytochromes (*2*), and photoactive yellow protein (PYP)[1] (*3*), respectively. In these proteins, an altered chromophore structure after isomerization enforces protein structural changes, followed by specific protein−protein interaction to activate transducer protein. However, such a general scheme needed to be reconsidered following the discovery of sensor proteins with flavins as the chromophore (*4*−*7*). How is light energy converted into protein structural changes for flavin-binding proteins so as to activate a transducer?

Phototropin (phot) is a blue-light receptor protein in plants involved in phototropism (*8*), chloroplast movement (*9*), and stomatal opening (*10*). Phot is composed of ∼1000 amino acid residues and two prosthetic flavin mononucleotide (FMN) molecules. The two FMN binding domains (ca. 100 residues) are named LOV (light-, oxygen-, and voltage-sensing) domains, which are a subset of the PAS (Per−Arnt−Sim) superfamily. In phot, the LOV1 and LOV2 domains are located in the N-terminal half, and the C-terminal half has a Ser/Thr kinase motif. Thus, the photochemical reaction of FMN yields kinase activation through a domain−domain interaction. LOV domains have characteristic absorptions at about 450 nm, so that they look yellow. Light absorption of FMN leads to the formation of a triplet excited state that absorbs at about 660 nm, where the intersystem crossing takes place in a few nanoseconds (*11*). Then, a ground-state intermediate is formed in a few microseconds that absorbs at 390 nm (S390 intermediate) (*12*). It is now known that the reaction is an adduct formation between FMN and a nearby cysteine (*12*−*17*). Since S390 is the sole intermediate in the photocycle of LOV domains, it is believed that S390 is the intermediate activating the kinase domain.

The photochemical property of adduct formation in phot is highly different from that of other light-sensor proteins initiated by photoisomerization. A remarkable aspect is the temperature dependence of the photoreaction. It is well-known that photoisomerization in rhodopsins, PYP, and phytochrome possesses little temperature dependence in terms of the reaction rate and efficiency. This indicates that the potential barrier of the reaction coordinate in the excited state is very low in these systems, so that the reactions are ultrafast events. Photoisomerization takes place even at cryogenic temperatures, where the protein environment is frozen. On the other hand, how is the adduct formation in phot influenced by temperature? In the case of the LOV2

* To whom correspondence should be addressed: phone/fax 81-52-735-5207; e-mail kandori@nitech.ac.jp.
[‡] Nagoya Institute of Technology.
[§] Tokyo Institute of Technology.
[||] Osaka Prefecture University.

[1] Abbreviations: PYP, photoactive yellow protein; phot, phototropin; FMN, flavin mononucleotide; LOV, light−oxygen−voltage; FTIR, Fourier transform infrared.

10.1021/bi701022v CCC: $37.00
Published on Web 08/17/2007

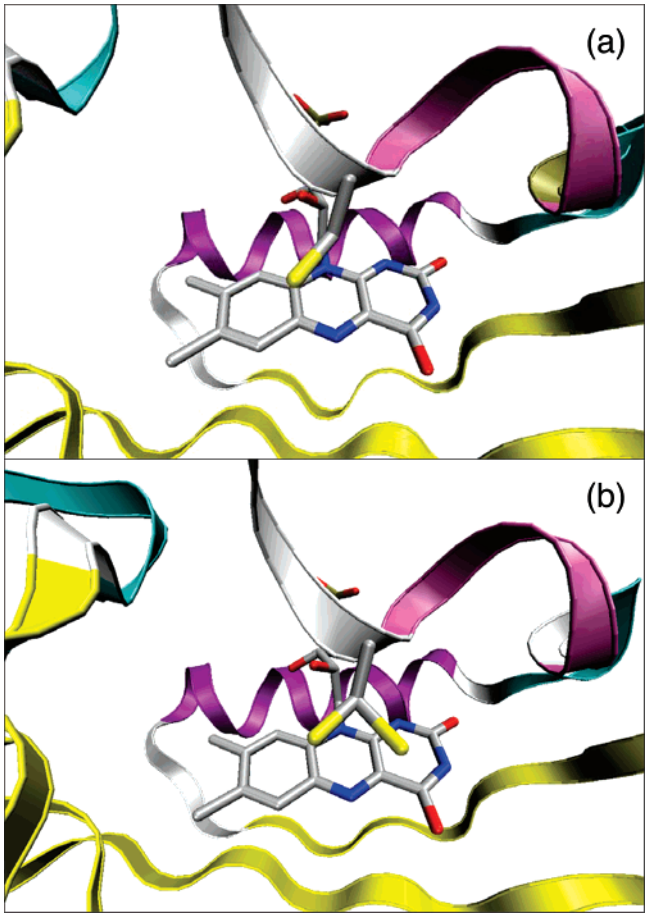

FIGURE 1: Protein structures near the FMN chromophores of (a) *Adiantum* neo1-LOV2 (PDB 1G28) (*14*) and (b) *Chlamydomonas* phot−LOV1 (PDB 1N9N) (*20*). FMN and the side chain of the reactive cysteine are shown by a stick drawing, whereas the remaining part is shown by a ribbon drawing. In panel a, the distance between the C4a atom of FMN and the sulfur atom of the cysteine (Cys966) is 4.2 Å. On the other hand, isomeric structures are observed for the cysteine (Cys57) in panel b, whose distances to the C4a atom of FMN are 3.5 and 4.4 Å.

domain of *Adiantum* neochrome1 (neo1-LOV2), a fusion protein of phot containing the phytochrome chromophoric domain, the distance between the C4a position of FMN and the sulfur atom of Cys966 is determined to be 4.2 Å by X-ray crystallography (Figure 1a) (*14*). Reduced reaction efficiency may be expected for phot at low temperatures, where the protein motion is frozen. Indeed, we found that S390 is formed at any temperature between 77 and 295 K for neo1-LOV2, whereas formation yield of S390 was reduced at low temperatures (*18*, *19*). The unreactive fractions were 64% and 36% at 77 and 100 K, respectively, suggesting that structural heterogeneity prohibits molecular motion for adduct formation at low temperatures.

Previous X-ray crystallography provided a hint of such structural heterogeneity. Although only one structure was reported for *Adiantum* neo1-LOV2 (*14*), isomeric forms of the reactive cysteine were found in the structure of *Chlamydomonas* phot-LOV1 (*20*). According to the structure, two distances, 3.5 and 4.4 Å, were reported between the C4a position of FMN and the sulfur atom of the cysteine in *Chlamydomonas* phot-LOV1 (Figure 1b) (*20*). This observation suggested the presence of multiple cysteine structures of LOV domains, which could explain the reduced adduct formation in LOV domains at low temperatures. We expect that the reaction is more efficient in the structure with a 3.5-Å distance than that with a 4.4-Å distance. Such multiple structures may be similarly present for *Adiantum* neo1-LOV2. However, Bednartz et al. (*21*) measured LOV domains from phot of *Chlamydomonas* by FTIR spectroscopy and showed that the structure of the cysteine residue is heterogeneous for LOV1 but homogeneous for LOV2. Does this apply to all LOV domains, including neo1-LOV2?

In this study, we aimed at obtaining spectroscopic evidence of structural heterogeneity for *Adiantum* neo1-LOV2. To achieve this, we focused the microenvironment of Cys966, the only cysteine present in *Adiantum* neo1-LOV2. The present low-temperature FTIR study successfully distinguished different protein structures by detecting S−H stretching vibrations at 77 and 150 K. There are two structures forming an adduct by illumination at 77 K. We found a structure that does not form an adduct at 77 K but rather at 150 K. Adduct formation is more efficient for the former two structures than for the latter. Molecular dynamics simulation strongly suggests that the observed multiple structures originate from the isomeric forms of Cys966. We thus concluded that there are multiple local structures of FMN and cysteine in neo1-LOV2, each of which is thermally converted by protein fluctuation at physiological temperatures.

MATERIALS AND METHODS

Sample Preparation. A fusion protein of *Adiantum* neo1-LOV2 with calmodulin-binding peptide (CBP) was prepared by using the pCAL-n-EK affinity protein expression and purification system (Stratagene). The construct contains N-terminal CBP and spans amino acid residues from Pro905 to Pro1087 of neo1, which include the Jα helix (Asp1050−Arg1072) (*22*, *23*). The neo1-LOV2 domain was expressed in *Escherichia coli* BL21(DE3) and was purified by a calmodulin affinity column as described previously (*18*, *19*). Purified protein was concentrated to 2 mg/mL and dialyzed against 1 mM potassium phosphate buffer (pH 7). The protein solution was placed on a BaF_2 window, and then dried to a film under reduced pressure with an aspirator. The dry film was hydrated by putting a drop of H_2O, D_2O, or $D_2{}^{18}O$ (Icon Isotopes; D 99%, ^{18}O 95%) next to the film on the BaF_2 window. This window was covered by another BaF_2 window with a greased spacer and sealing film.

Spectroscopy. UV−Visible and infrared spectra of the hydrated films were measured on V-550DS (Jasco) and FTS-40 (Bio-Rad) spectrophotometers, respectively. Low-temperature spectra were measured by use of a cryostat (Optistat DN, Oxford) and a temperature controller (ITC 4, Oxford) with liquid nitrogen as coolant. The data are presented as difference spectra, after and before illumination of the sample with >400 nm light, which was supplied with a combination of a halogen−tungsten lamp (1 kW) and a long-pass filter (L42, Asahi Techno Glass). For FTIR spectra, 256 interferograms at 2 cm^{-1} resolution were recorded before and after illumination and 8−10 recordings were averaged.

Calculations. The starting configuration of neo1-LOV2 was derived from the X-ray structure, 1G28, in the Protein Data Bank. The AMBER96 all-atom force field (*24*) and the TIP3P model were used for the protein part of neo1-LOV2 and for water, respectively. The force-field parameters for FMN were taken from the AMBER96 parameter database

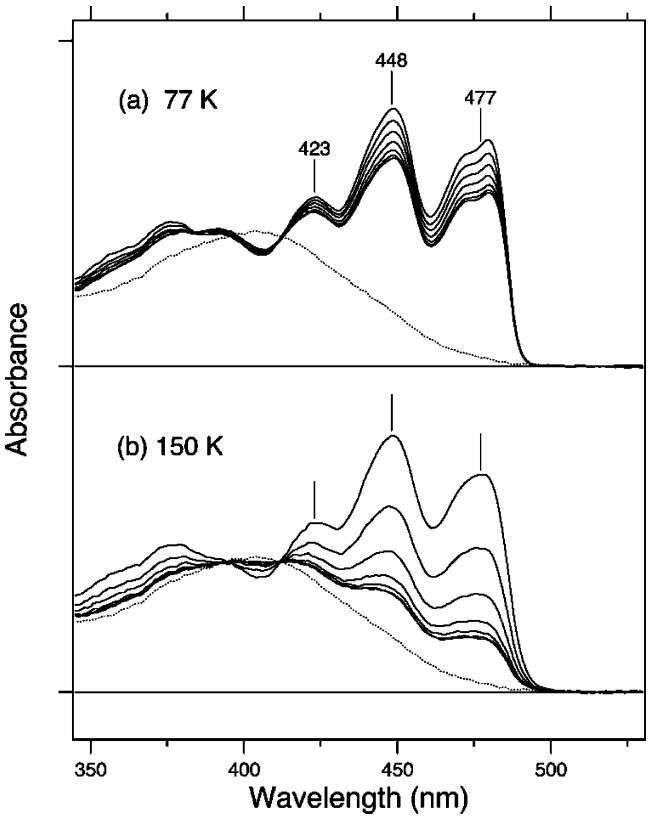

FIGURE 2: UV−visible spectral changes upon light illumination of neo1-LOV2 at (a) 77 and (b) 150 K.. Solid lines represent the spectra of the unphotolyzed state, and absorption at 450−500 nm decreases by illuminating for 2, 5, 10, 20, 40, and 60 s (thin solid lines). Dotted lines represent the calculated spectra of S390.

(*24*). However, the atomic charges of FMN were determined so as to fit the results of B3LYP/6-31G* calculations. The protein was solvated in a water droplet with a radius of 33 Å around the protein molecule. The net charge of −2.0 was compensated by adding two sodium ions into the system. Furthermore, 15 sodium ions and 13 chloride ions were added. The resulting ion concentration was approximately 0.15 M. The ions were set by randomly replacing water molecules. Consequently, the system studied contained 14 752 atoms. After an energy minimization starting from this initial system, the temperature was gradually increased from 0 to 300 K during 1 ns and an additional simulation was done for a 100 ps at 300 K so as to equilibrate the system. Subsequently, a 12 ns simulation was done at 300 K for data sampling. The temperature was controlled using the Nosé−Hoover algorithm (*25*, *26*). The other simulation conditions were as follows: the time step of the numerical integration was 1 fs; all heavy atom−hydrogen atom bonds were held rigid by the SHAKE algorithm (*27*); and electrostatic interactions were calculated by a cell multipole method. Coordinate trajectories were stored at a rate of 10/ps. The simulation was carried out with the MD simulation program PRESTO, version 3 (*28*).

RESULTS AND DISCUSSION

Low-Temperature UV−Visible Spectra of Neo1-LOV2. Figure 2 shows UV−visible absorption spectra of neo1-LOV2 and their changes upon illumination at 77 K (a) and at 150 K (b). Absorption spectra of neo1-LOV2 possess three peaks at 423, 448, and 477 nm, characteristic of the absorption of FMN. Illumination with >400 nm light then reduced the peaks accompanying the formation of S390 (Figure 2). Such transitions exhibit isosbestic points at each temperature (such as 395 and 412 nm), and shapes of difference spectra are identical among various illumination times, indicating that the transition can be described by a single conversion of neo1-LOV2 to S390. Nevertheless, almost no further reduction was observed. Reactive fractions were estimated to be 28% and 78% at 77 and 150 K, respectively. Presence of the unreactive fraction originates from neither (i) thermal reversion nor (ii) photoreversion from S390 to the original state, because S390 was stable at ≤250 K, and the same results were obtained by illumination with longer wavelengths (data not shown). Thus, neo1-LOV2 has a fraction that does not form S390, as we previously reported (*18*, *19*).

The incomplete conversion of neo1-LOV2 to S390 at these low temperatures is presumably due to freezing of molecular motions around FMN. Conformation of neo1-LOV2 in the unphotolyzed state must fluctuate in solution at ambient temperatures, where the distance between the cysteine S−H group and C4a of FMN is changing rapidly. The distance of 4.2 Å in the crystal structure (*14*) represents the most stable state in that crystal. Enhanced dynamical motions at higher temperatures enable neo1-LOV2 to form the cysteinyl−flavin adduct. However, reduced molecular motions at 77 and 150 K may hinder adduct formation. If this is the case, neo1-LOV2 should have various distributions on the local structures around FMN. Therefore, we next examined local structures at low temperatures by means of FTIR spectroscopy, particularly focusing the microenvironment of Cys966.

Low-Temperature FTIR Spectra of Neo1-LOV2 in the 2610−2530 cm^{-1} Region. Figure 3a (thick solid line) shows a light-minus-dark difference IR spectrum of neo1-LOV2 in the S−H stretching region at 77 K. As we reported previously (*18*), a negative peak appears at 2569 cm^{-1}, which is absent in the baseline (thin solid line). Since neo1-LOV2 has only one cysteine, the S−H stretching vibration comes from Cys966. The absence of respective positive bands is consistent with the adduct formation of the S−H group with FMN. It is noted that the negative band is not symmetrical in spectral shape, and it is more broadened at the low-frequency side (2569−2540 cm^{-1}). This suggests that the structure of the S−H group is not homogeneous at 77 K.

Under the present conditions (77 K), 28% of neo1-LOV2 was photoconverted to S390, while the remaining 72% was insensitive to further light illumination (Figure 2a). In contrast, 78% of neo1-LOV2 was photoconverted to S390 at 150 K (Figure 2b). Therefore, we next tried the following measurement. We first illuminated the sample at 77 K and then illuminated at 150 K after warming. We expected that the subsequent illumination at 150 K yields the difference spectra for the protein structures that are unreactive at 77 K but reactive at 150 K. Figure 3b (thick solid line) shows the corresponding light-minus-dark spectrum, which is different from the solid line in Figure 3a. The peak frequency is 2564 cm^{-1}, and the spectral shape is symmetrical. It should be noted that the spectrum in Figure 3b is also different from that at 150 K without preillumination (thick solid line in Figure 3c), which possesses a peak frequency at 2567 cm^{-1} and a nonsymmetrical spectral shape. These results strongly suggest that the local structure of Cys966 is different between the reactive and unreactive fractions at 77 K. The dotted line in Figure 3c is the sum of the thick, solid lines of Figure 3

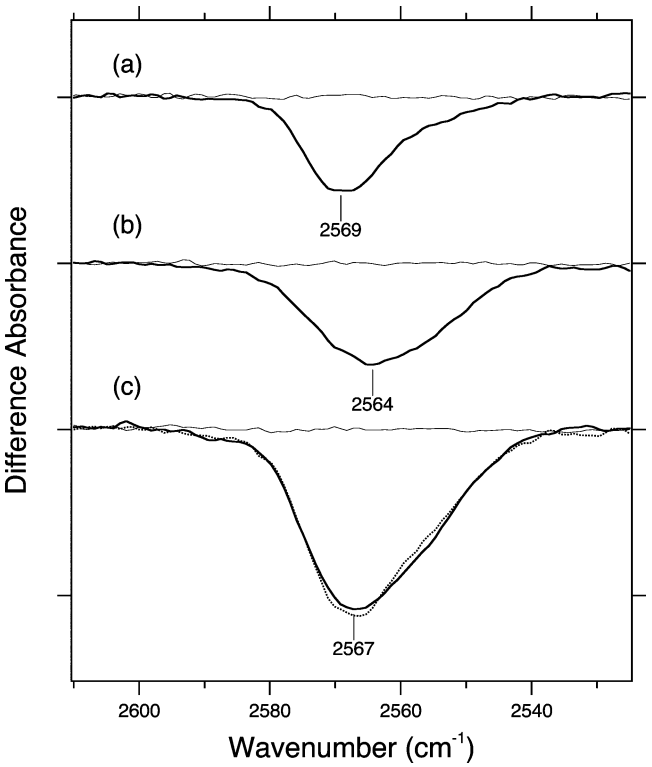

FIGURE 3: Light-minus-dark (thick solid lines) and dark-minus-dark (thin solid lines) FTIR difference spectra for neo1-LOV2 in the 2610−2530 cm^{-1} region. (a) FTIR spectra at 77 K, where 28% of neo1-LOV2 is photoconverted to S390. (b) FTIR spectra at 150 K after the measurement at 77 K (Figure 3a). This measurement at 150 K was done after warming from 77 K and being incubated for 60 min, indicating that the spectra correspond to those unreactive at 77 K but reactive at 150 K. (c) Thick solid line represents the FTIR spectra at 150 K, while the dotted line is the sum of thick solid lines of panels a and b. One division of the *y*-axis corresponds to 0.0004 absorbance unit.

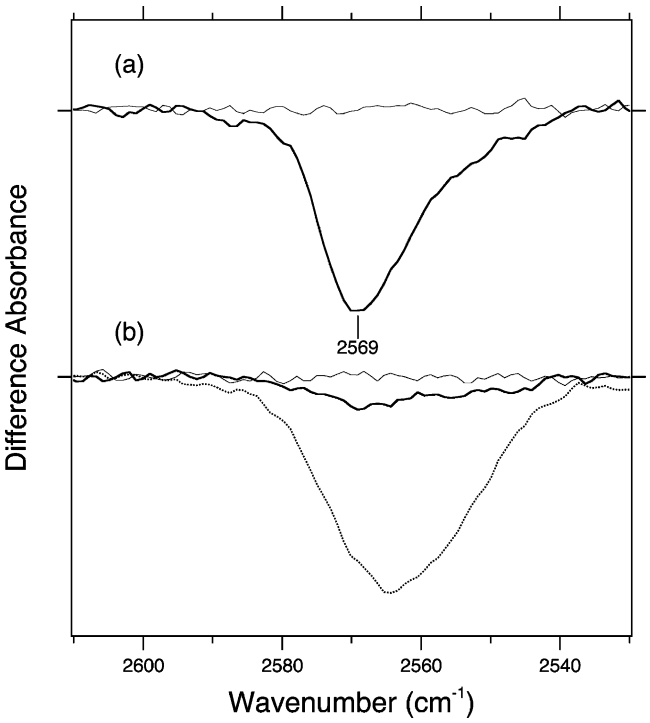

FIGURE 4: (a) Light-minus-dark (thick solid lines) and dark-minus-dark (thin solid lines) FTIR spectra at 77 K, reproduced from Figure 3a. (b) Solid lines represent the following measurement. After the measurement in panel a, the sample was incubated for 60 min at 150 K, followed by recooling at 77 K. If the reactive and unreactive components at 77 K are in equilibrium at 150 K, this procedure converts the unreactive component to be reactive at 77 K. Thick and thin solid lines correspond to the light-minus-dark and dark-minus-dark FTIR spectra at 77 K, respectively. For comparison, the spectrum of Figure 3b (thick solid line) is reproduced as a dotted line. One division of the *y*-axis corresponds to 0.0003 absorbance unit.

panels a and b. Spectral coincidence between solid and dotted lines in Figure 3c excludes the possibility that the different spectral shapes are owing to the effect of temperature.

It is noted, however that protein fluctuation significantly depends on temperature, and fluctuation at 150 K must be more than that at 77 K. Therefore, the reactive fraction at 77 K might emerge by warming from 77 to 150 K, which disturbs the present analysis. Figure 4 examines such a possibility. Figure 4a shows the light-minus-dark difference IR spectrum of neo1-LOV2 at 77 K, being reproduced from Figure 3a. By warming the sample from 77 to 150 K, additional spectral changes take place by illumination at 150 K (dotted line in Figure 4b; reproduced from Figure 3b). In the measurement of Figure 4, the sample was not illuminated but was incubated for 60 min at 150 K. After incubation, the sample was cooled down from 150 to 77 K. The thick, solid line in Figure 4b is the difference spectrum by the following illumination at 77 K. We observed a small amount of negative band, indicating that incubation at 150 K converts the unreactive fraction into a reactive one at 77 K by protein fluctuation. Nevertheless, the amount was less than 10%, and we concluded that such a conversion is negligible in the present analysis. In other words, local environments of the S−H group of Cys966 are structurally frozen at 77−150 K.

In this study, we define the three states as follows. States I, II, and III stand for the reactive component at 77 K (28%), the component unreactive at 77 K but reactive at 150 K (50%), and the unreactive component at 150 K (22%), respectively. We observed characteristic S−H stretching vibrations for states I and II (Figure 3). It is also interesting to compare the FTIR spectra in another frequency region. However, there were no clear differences for states I and II in the 1800−1000 cm^{-1} region except for the amide I vibration (data not shown), which exhibits temperature dependence between 77 and 150 K (*18*). This suggests that protein structures are almost identical between states I and II.

Spectral Analysis of the S−H Stretching Vibration. At low temperatures, some S−H bands are symmetrical, while others are not. Therefore, we attempted to constitute the experimental data by use of Gaussian curve fitting. Dotted lines in Figure 5a show Gaussian functions whose peak frequencies are 2569.6 (±0.1) and 2562.3 (±0.6) cm^{-1}, and the sum coincides well with the experimental data (solid line in Figure 5a). Full widths of the half-maxima of the bands at 2569.6 and 2562.3 cm^{-1} are 14.3 and 27.5, respectively, and the area of the 2569.6-cm^{-1} band is 0.95 times larger than that of the 2562.3-cm^{-1} band. Thus, the negative band at 77 K (Figure 3a) can be composed of two bands possessing Gaussian spectral shapes. This fact suggests that state I is composed of two different substates for the reactive cysteine. In contrast, the dotted line in Figure 5b is a single Gaussian curve whose peak frequency is 2563.0 (±2.3) cm^{-1}. The Gaussian curve coincides well with the experimental data that is unreactive at 77 K but reactive at 150 K (solid line in Figure 5b; reproduced from thick solid line in Figure 3b),

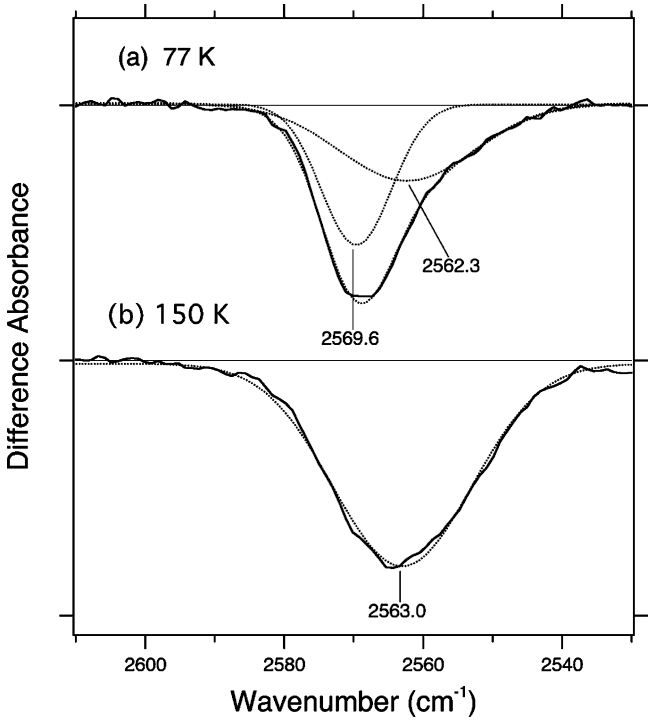

FIGURE 5: Gaussian curve fittings (dotted lines) of the S−H stretching vibrations at (a) 77 and (b) 150 K. Thick solid lines in panels a and b are reproduced from the corresponding panels in Figure 3, respectively. One division of the *y*-axis corresponds to 0.0003 absorbance unit.

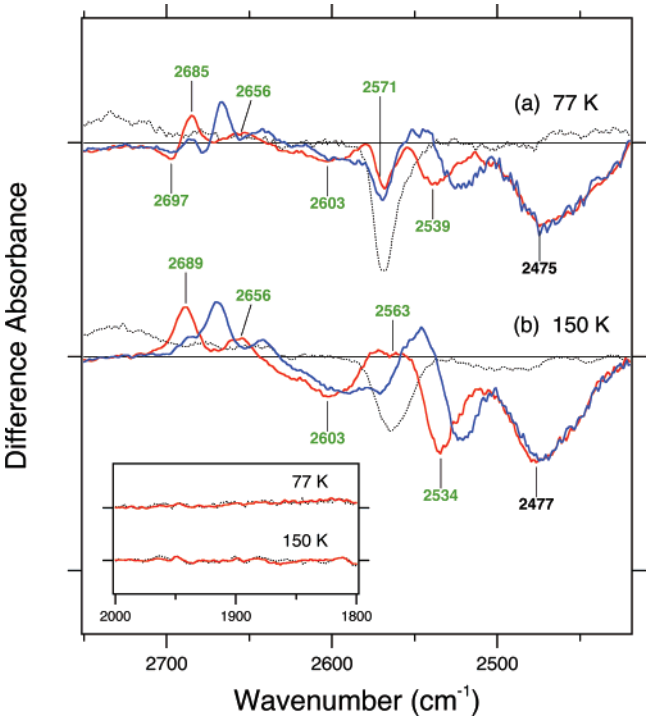

FIGURE 6: Light-minus-dark FTIR difference spectra for neo1-LOV2 in the 2750−2420 cm^{-1} region. (a) FTIR spectra at 77 K, where 28% of neo1-LOV2 is photoconverted to S390. (b) FTIR spectra at 150 K after the measurement at 77 K (panel a). Red and blue lines represent the spectra in D_2O and $D_2{}^{18}O$, respectively. Dotted lines in panels a and b are reproduced from thick, solid lines in the corresponding panels in Figure 3, respectively. Green labeled frequencies correspond to those identified as water-stretching vibrations. One division of the *y*-axis corresponds to 0.0007 absorbance unit. (Inset) Light-minus-dark FTIR difference spectra for neo1-LOV2 in the 2000−1800 cm^{-1} region. One division of the *y*-axis corresponds to 0.00025 absorbance unit.

indicating that the S−H group of Cys966 is located in a single environment.

S−H stretching vibrations appear in the 2580−2525 cm^{-1} region and their frequencies decrease as the hydrogen bonding of the S−H groups becomes stronger. Therefore, the frequency of 2570 cm^{-1} indicates that the S−H group is almost free from hydrogen bonds. In contrast, the frequencies at 2562 and 2563 cm^{-1} correspond to weak hydrogen bonds. Thus, state I possesses two conformations of the S−H group of Cys966, one of which is similar to that in state II in terms of hydrogen-bonding strength.

Low-Temperature FTIR Spectra of Neo1-LOV2 in the 2750−2420 cm^{-1} Region. O−D stretching vibrations of D_2O appear in the 2700−2200 cm^{-1} region, which depend on their hydrogen-bonding strengths. In general, the frequency is lowered when the hydrogen bond is strengthened. Figure 6a shows the light-minus-dark difference IR spectra of neo1-LOV2 at 77 K, where red and blue lines correspond to the spectra in D_2O and $D_2{}^{18}O$, respectively. In the 2750−2420 cm^{-1} region, a clear isotope shift of water was observed, whereas no water bands were shown in the <2420 cm^{-1} region (data not shown). The spectrum at 77 K exhibits three negative O−D stretches of water at 2697, 2603, and 2539 cm^{-1} (Figure 6a), suggesting that at least two water molecules in state I change their hydrogen bonds. Dotted lines show the light-minus-dark difference IR spectrum of neo1-LOV2 in H_2O, reproduced from Figure 3a. As shown in the inset of Figure 6, the S−H stretch of Cys966 is not deuterated, and the red and blue spectra are largely perturbed in the 2590−2540 cm^{-1} region. In addition to the positive bands at 2685 and 2656 cm^{-1}, we suggest the presence of a positive 2571-cm^{-1} band, because subtraction of the dotted line clearly showed the positive water band (data not shown).

Figure 6b shows the light-minus-dark spectra at 150 K after the measurement at 77 K, which corresponds to state II. The spectral feature in Figure 6b clearly differs from that of Figure 6a. The negative band at 2697 cm^{-1} in Figure 6a disappears in Figure 6b. In addition, the negative band at 2534 cm^{-1} in Figure 6b is more intense than the 2539-cm^{-1} band in Figure 6a, suggesting the presence of two O−D stretches at 2534 cm^{-1}. It is likely that the O−D stretch of water at 2697 cm^{-1} in the structure of state I downshifts to 2534 cm^{-1} in the structure of state II. From the frequency, state I possesses a water molecule that is almost free from hydrogen bonds, whereas the water molecule forms a hydrogen bond in state II.

Neo1-LOV2 has two internal water molecules, Wat25 and Wat45, near FMN (*14*). Wat45 is closer to FMN and Cys966, but the distance between Wat45 and the sulfur atom of Cys966 (4.4 Å) suggests no hydrogen bond according to the crystal structure. Nevertheless, Wat45 may be able to form a hydrogen bond with Cys966 in a local structure, and molecular dynamics simulation indeed implies such a direct hydrogen-bonding interaction between Wat45 and Cys966 in one conformer state, presumably state II (see below).

Quantum Efficiencies in Formation of the S390 Intermediate for Different States. We next compared quantum efficiencies in formation of S390 for each structural fraction. The S390 intermediates formed are thermally reverted to the original states at room temperature, whereas we found that

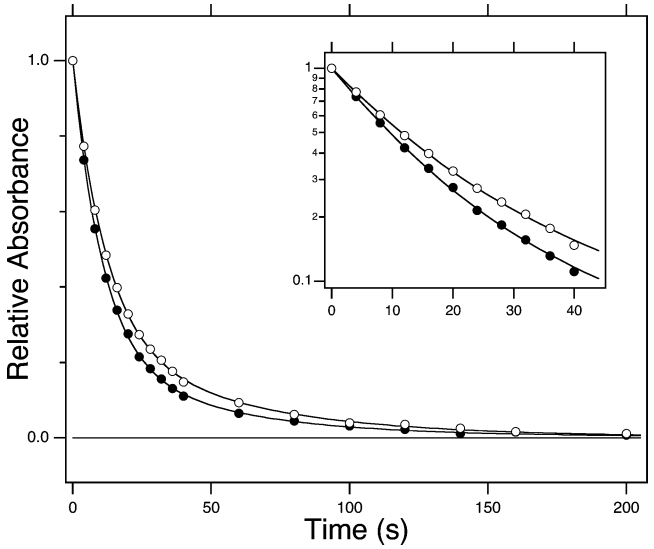

FIGURE 7: Time course of the photoconversion of neo1-LOV2 to the S390 intermediate measured at 150 K, (○) with or (●) without preillumination at 77 K. The *y*-axis corresponds to the remaining reactive fraction, which is estimated from the absorbance at 475 nm. Smooth lines are double-exponential fitting curves; the inset shows their logarithmic plots.

S390 is stable at ≤250 K. Figure 7 plots the bleached LOV domains versus illumination time at 150 K, where the decay "rate" has a correlation with the photosensitivity of the photoconversion to S390, namely adduct formation. Open circles in Figure 7 represent the measurement with preillumination at 77 K, which corresponds to state II. On the other hand, filled circles represent measurements without any preillumination, which corresponds to states I and II. Figure 7 clearly shows that the latter state is more photosensitive than the former, implying that the reactive fraction at 77 K (state I) is more efficient in adduct formation than the unreactive fraction at 77 K (state II). It would be reasonable to assume that the efficient component in adduct formation is reactive at lower temperatures. This fact may suggest that the distance between FMN and Cys966 is closer for the reactive fraction at 77 K (state I).

Both time courses could not be fitted by single exponentials, which is clearly shown in the logarithmic plot (Figure 7, inset). It is reasonable that the filled circles are not fitted by a single exponential, because there are multiple structures at 150 K (Figure 3c). In contrast, open circles are not fitted by a single exponential even though the structure of the S−H group can be described by a single state. This suggests the reaction trajectory in the excited (singlet and triplet) states to be multiple. Namely, there are possibly multiple states (structures) in the triplet excited state, even when the neo1-LOV2 molecule is excited from a single structure.

Conformation Analysis for the Active Site and Interpretation of Experimental Data. To examine the conformational distributions of the active site including FMN and the side chain of Cys966, the MD trajectories for 10 ns were analyzed. Figure 8 shows the time evolutions of two dihedral angles of Cys966, (a) χ_1(N−C_α−C_β−S) and (b) χ_2 (C_α−C_β−S−H). These data show that χ_1 is distributed between two local minima (−60° ± 20° and −150° ± 20°) and χ_2 among four local minima (50° ± 50°, −40° ± 20°, −140° ± 10°, and −240° ± 20°). Interestingly, when χ_1 is −60° ± 20°, χ_2 is either 50° ± 50° or −40° ± 20°, and when χ_1 is

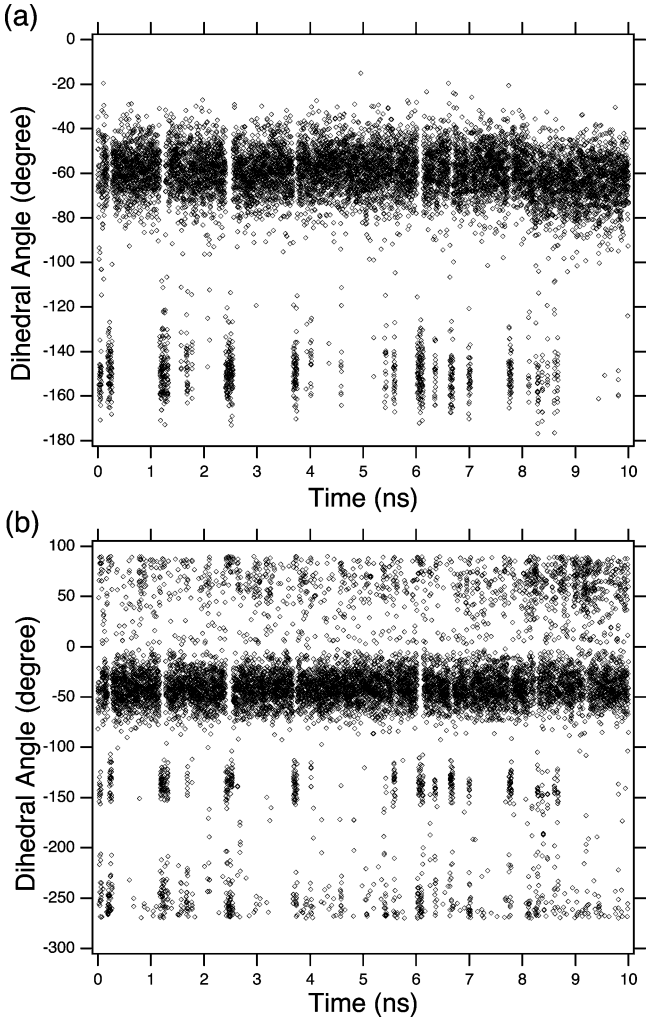

FIGURE 8: Time dependence of two dihedral angles of the Cys966 side chains: (a) χ_1 (N−C_α−C_β−S) and (b) χ_2 (C_α−C_β−S−H).

−150° ± 20°, χ_2 is either −140° ± 10° or −240° ± 20°. Thus, the side chain of Cys966 takes four types of conformations as shown in Figure 9. In conformers A and B, the sulfur atom of Cys966 is positioned just above the N5 atom of FMN with a short distance of 3.0 Å; in the former and latter, the SH group of Cys966 forms hydrogen bonds with the carbonyl oxygen of Cys966 and the N5 atom of FMN, respectively. In conformers C and D, the sulfur atom of Cys966 is somewhat distant from the N5 atom of FMN (>3.8 Å), and interestingly the SH group of conformer D forms a hydrogen bond with Wat45. The populations of the four conformers at 300 K were calculated for a total of 10 000 snapshots that were randomly selected from the 10 ns trajectory data. As a result, the populations of conformers A, B, C, and D were 4.4%, 5.0%, 14.1%, and 76.6%, respectively. These computational results strongly support the present experimental observation, in which the environment of Cys966 is highly heterogeneous.

It has been proposed that in the initial step of adduct formation the thiol hydrogen of Cys966 is abstracted by the N5 atom of FMN, followed by nucleophilic attack of the sulfide on the C4a atom to form the covalent bond between the C4a atom of FMN and the thiol sulfur atoms (*14*, *20*). Such an initial reaction would be possible only through the formation of conformer B (Figure 9B). At ambient temperature, the four conformers A−D are in equilibrium with each

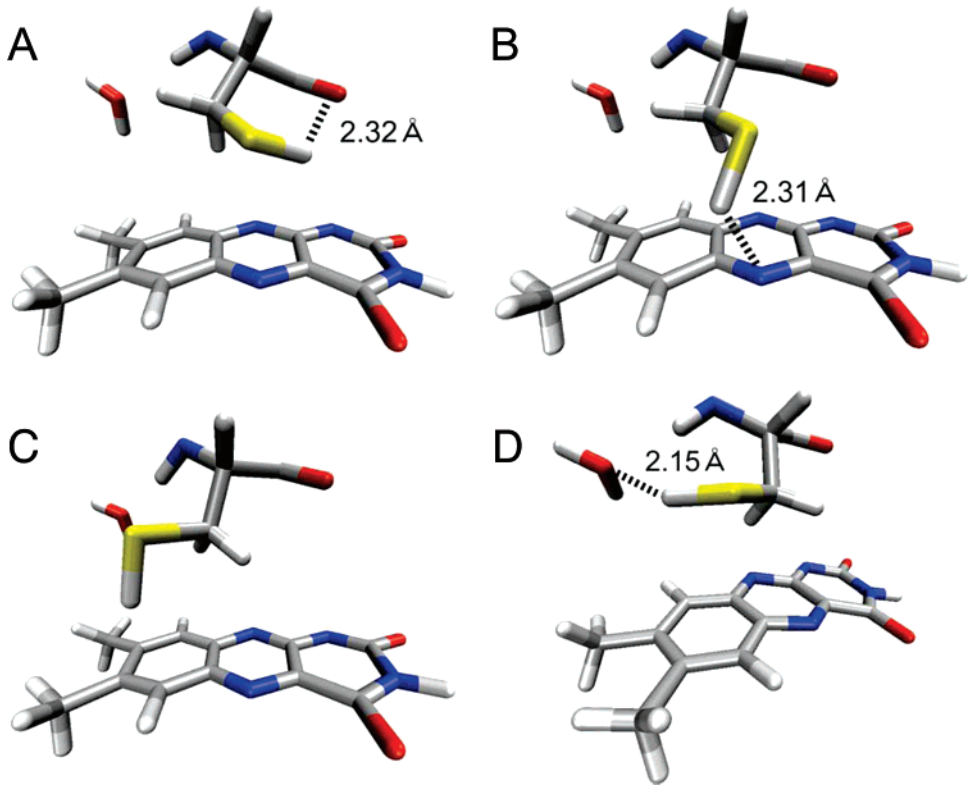

FIGURE 9: Snapshots showing the four possible conformations of the Cys966 side chain with the isoalloxazine ring of FMN and water45 in the dark state. Red, oxygen; blue, nitrogen; green, carbon; yellow, sulfur; white, hydrogen. The distance for the characteristic hydrogen bond found in each conformer is shown.

other. Upon illumination, conformer B is first converted into the product, but it could be provided almost instantly through the rapid exchange reactions among the four conformers. Thus, the photochemical reaction continues until they are completely consumed. With lowering temperature, the rates of such exchange reactions decrease and then reaction steps with large activation energies occur with difficulty, leading to the appearance of unreactive components. Indeed, according to Figure 3, there is at least one component that is unreactive at 77 K but reactive at 150 K.

We next attempted to interpret the temperature dependence of adduct formation (Figures 2−7) on the basis of the computational analysis. The reactive state at 77 K (state I) consists of at least two components differing in the thiol S−H stretching vibrations (Figure 5). The component at 2562.3 cm^{-1} corresponds to a conformer that forms a hydrogen bond with its neighboring group(s), while that at 2569.6 cm^{-1} should be assigned to a conformer almost free from a hydrogen bond. Among the four conformers, conformers A and B are different only in the orientation of the SH bond (torsion around the C_β−S bond) and thereby they are rapidly interconverted into each other even at low temperatures. This implies that both conformers behave as if they were one component. In addition, their thiol groups form hydrogen bonds with the neighboring groups (Figure 9A,B). Taken together, it is reasonable to interpret that state I possessing the S−H stretch at 2562.3 cm^{-1} consists of conformers A and B. The sum of populations of comformers A and B (4.4% + 5.0% = 9.4%) is close to the experimental value (14%). On the other hand, state I possessing the S−H stretch at 2569.6 cm^{-1} is possibly assigned to conformer C, because the SH group is free from a hydrogen bond only in this conformer (Figure 9C). The computational population of comformer C (14.1%) is identical to the experimental value (14%).

The conversion into conformer D seems to take place with a higher activation energy because its structure is more distorted compared to the other conformers. This implies that a higher temperature is required to produce conformer D, probably corresponding to the component that becomes reactive at 150 K (state II). As shown in Figure 9D, the SH group of conformer D is hydrogen-bonded with Wat45. The newly formed hydrogen bond between Cys966 and Wat45 probably affects the frequency of Wat45, which corresponds to the different water O−D stretches between states I and II. Therefore, it can be safely said that the main component of state II is conformer D.

CONCLUSION

In the biological light-signal transduction initiated by cis−trans photoisomerization of chromophore molecules, an altered chromophore structure after isomerization enforces protein structural changes, followed by specific protein−protein interactions to activate transducer protein. Mechanism of light energy storage for flavin-binding proteins is of interest. The primary reaction in phototropin is adduct formation between FMN and a nearby cysteine (*12*−*17*), where the altered chromophore−protein interaction must drive subsequent protein structural changes. The distance between the C4a position of FMN and the sulfur atom of Cys966 (4.2 Å) in neo1-LOV2 requires protein fluctuation for the adduct formation. While such a distance may be advantageous for light energy storage as the structural constraint in protein, we found that adduct formation is

significantly reduced at low temperatures (64% and 36% are unreactive at 77 and 100 K, respectively) (*18*). This observation suggested structural heterogeneity, although the detailed structural feature remains unknown. The present low-temperature FTIR study successfully distinguished different protein structures by detecting S−H stretching vibrations at 77 and 150 K. There are two structures forming an adduct by illumination at 77 K (28%; state I). We found a structure that does not form an adduct at 77 K but forms one at 150 K (50%; state II), and 22% was unreactive at 150 K (state III). FTIR spectroscopy further revealed different hydrogen-bonding conditions of the SH group of Cys966 and nearby water. MD simulation combined well the structure and IR observation, where the observed multiple structures originate from the isomeric forms of Cys966.

ACKNOWLEDGMENT

We thank D. Nozaki for his experimental assistance.

REFERENCES

1. Kandori, H., Shichida, Y., and Yoshizawa, T. (2001) Photoisomerization in Rhodopsin, *Biochemistry (Moscow) 66*, 1197−1209.
2. Andel, F., III, Murphy, J. T., Haas, J. A., McDowell, M. T., van der Hoef, I., Lugtenburg, J., Lagarias, J. C., and Mathies, R. A. (2000) Probing the Photoreaction Mechanism of Phytochrome through Analysis of Resonance Raman Vibrational Spectra of Recombinant Analogues, *Biochemistry 39*, 2667−2676.
3. Hellingwerf, K. J., Hoff, W. D., and Crielaard, W. (1996) Photobiology of microorganisms: how photosensors catch a photon to initialize signalling, *Mol. Microbiol. 21*, 683−693.
4. Cashmore, A. R., Jarillo, J. A., Wu, Y. J., and Liu, D. (1999) Cryptochromes: blue light receptors for plants and animals, *Science 284*, 760−765.
5. Huala, E., Oeller, P. W., Liscum, E., Han, I. S., Larsen, E., and Briggs, W. R. (1997) *Arabidopsis* NPH1: a protein kinase with a putative redox-sensing domain, *Science 278*, 2120−2123.
6. Iseki, M., Matsunaga, S., Murakami, A., Ohno, K., Shiga, K., Yoshida, K., Sugai, M., Takahashi, T., Hori, T., and Watanabe, M. (2002) A blue-light-activated adenylyl cyclase mediates photoavoidance in *Euglena gracilis*, *Nature 415*, 1047−1051.
7. Lin, C. (2000) Plant blue-light receptors, *Trends Plant Sci. 5*, 337−342.
8. Liscum, E., and Briggs, W. R. (1995) Mutations in the *NPH1* Locus of *Arabidopsis* Disrupt the Perception of Phototropic Stimuli, *Plant Cell 7*, 473−485.
9. Kagawa, T., Sakai, T., Suetsugu, N., Oikawa, K., Ishiguro, S., Kato, T., Tabata, S., Okada, K., and Wada, M. (2001) *Arabidopsis* NPL1: A Phototropin Homolog Controlling the Chloroplast High-Light Avoidance Response, *Science 291*, 2138−2141.
10. Kinoshita, T., Doi, M., Suetsugu, N., Kagawa, T., Wada, M., and Shimazaki, K. (2001) phot1 and phot2 mediate blue light regulation of stomatal opening, *Nature 414*, 656−660.
11. Kennis, J. T. M., Crosson, S., Gauden, M., van Stokkum, I. H. M., Moffat, K., and van Grondelle, R. (2003) Primary Reactions of the LOV2 Domain of Phototropin, a Plant Blue-Light Photoreceptor, *Biochemistry 42*, 3385−3392.
12. Salomon, M., Christie, J. M., Knieb, E., Lempert, U., and Briggs, W. R. (2000) Photochemical and Mutational Analysis of the FMN-Binding Domains of the Plant Blue Light Receptor, Phototropin, *Biochemistry 39*, 9401−9410.
13. Miller, S. M., Massey, V., Ballou, D., Williams, C. H., Jr., Distefano, M. D., Moore, M. J., and Walsh, C. T. (1990) Use of a site-directed triple mutant to trap intermediates: Demonstration that the flavin C(4a)-thiol adduct and reduced flavin are kinetically competent intermediates in mercuric ion reductase, *Biochemistry 29*, 2831−2841.
14. Crosson, S., and Moffat, K. (2001) Structure of a flavin-binding plant photoreceptor domain: Insights into light-mediated signal transduction, *Proc. Natl. Acad. Sci. U.S.A. 98*, 2995−3000.
15. Swartz, T. E., Corchnoy, S. B., Christie, J. M., Lewis, J. W., Szundi, I., Briggs, W. R., and Bogomolni, R. A. (2001) The Photocycle of a Flavin-Binding Domain of the Blue Light Photoreceptor Phototropin, *J. Biol. Chem. 276*, 36493−36500.
16. Salomon, M., Eisenreich, W., Dürr, H., Schleicher, E., Knieb, E., Massey, V., Rüdiger, W., Muller, F., Bacher, A., and Richter, G. (2001) An optomechanical transducer in the blue light receptor phototropin from *Avena sativa*, *Proc. Natl. Acad. Sci. U.S.A. 98*, 12357−12361.
17. Crosson, S., and Moffat, K. (2002) Photoexcited Structure of a Plant Photoreceptor Domain Reveals a Light-Driven Molecular Switch, *Plant Cell 14*, 1067−1075.
18. Iwata, T., Nozaki, D., Tokutomi, S., Kagawa, T., Wada, M., and Kandori, H. (2003) Light-Induced Structural Changes in the LOV2 Domain of *Adiantum* Phytochrome3 Studied by Low-Temperature FTIR and UV-Visible Spectroscopy, *Biochemistry 42*, 8183−8191.
19. Nozaki, D., Iwata, T., Tokutomi, S., and Kandori, H. (2005) Unique temperature dependence in the adduct formation between FMN and cysteine S-H group in the LOV2 domain of *Adiantum* phytochrome3, *Chem. Phys. Lett., 410*, 59−63.
20. Fedorov, R., Schlichting, I., Hartmann, E., Domratcheva, T., Fuhrmann, M., and Hegemann, P. (2003) Crystal structures and molecular mechanism of a light-induced signaling switch: The Phot-LOV1 domain from *Chlamydomonas reinhardtii*, *Biophys. J. 84*, 2474−2482.
21. Bednartz, T., Losi, A., Gärtner, W., Hegemann, P., and Heberle, J (2004) Functional vibrations among LOV domains as revealed by FT-IR difference spectroscopy, *Photochem. Photobiol. Sci. 3*, 575−579.
22. Harper, S. M., Neil, L. C., and Gardner, K. H. (2003) Structural basis of a phototropin light switch, *Science 301*, 1541−1544.
23. Harper, S. M., Christie, J. M., and Gardner, K. H. (2004) Disruption of the LOV-Jα Helix Interaction Activates Phototropin Kinase Activity, *Biochemistry 43*, 16184−16192.
24. Cornell, W. D., Cieplak, P., Bayly, C. I., Gould, I. R., Merz, K. M., Ferguson, D. M., Spellmeyer, D. C., Fox, T., Caldwell, J. W., and Kollman, P. A. (1995) A Second Generation Force Field for the Simulation of Proteins, Nucleic Acids, and Organic Molecules, *J. Am. Chem. Soc. 117*, 5179−5197.
25. Nosé, S. (1984) A molecular dynamics method for simulations in the canonical ensemble, *Mol. Phys. 52*, 255−268.
26. Hoover, W. G. (1985) Canonical dynamics: Equilibrium phase-space distributions, *Phys. Rev. A 31*, 1695−1697.
27. Ryckaert, J. P., Giccotti, G., and Berendsen, H. J. C. (1977) Numerical integration of the cartesian equations of motion of a system with constraints: molecular dynamics of *n*-alkanes, *J. Comput. Phys. 23*, 327−341.
28. Morikami, K., Nakai, T., Kidera, A., Saito, M., and Nakamura, H. (1992) PRESTO: A vectorized molecular mechanics program for biopolymers, *Comput. Chem. 16*, 243−248.

BI701022V